ELSEVIER

Interfacial engineering for high performance organic photovoltaics

Chao Yi[1], Xiaowen Hu[1], Xiong Gong[1,*] and Ahmed Elzatahry[2]

[1] Department of Polymer Engineering, The University of Akron, 44325, USA
[2] Materials Science and Technology Program, College of Arts and Sciences, Qatar University, PO Box 2713, Doha, Qatar

In the past two decades, bulk heterojunction (BHJ) organic photovoltaics (OPVs) have gained tremendous attention due to its intrinsic merits of cheap, flexible, clean and high throughput manufacturing processibility and its advanced features of short payback time. Various methodologies have been developed to approach OPVs with high power conversion efficiencies (PCEs) and long-term stability. Interfacial engineering is a proven efficient approach to achieve OPVs with high PCEs. In this article, we provide a basic overview on the recent progress of the materials, in particular, water/alcohol soluble organic materials, used as interfacial layer (IFLs) in engineering of BHJ OPVs with high PCEs. Underlying device physics of interfacial engineering and the origins of enhanced PCEs of OPVs by IFLs are highlighted.

Introduction

To take advantages of the unlimited solar energy, photovoltaic (PV) technology was developed [1]. Currently, inorganic PVs (IPVs) have been widely employed due to its high power conversion efficiencies (PCEs) and good stability [2]. However, IPVs are limited by the long payback time and the pollutions generated during the manufacturing processes [2]. Thus, IPVs cannot be considered as the green energy sources [3]. In contrast to IPVs, organic PVs (OPVs) as alternative to IPVs, features short payback time and low waste/pollution generation during device fabrication, becoming one of the green energy sources [4–9]. In the last two decades, scientists and engineers have dedicated significant efforts on development of novel materials [13–20], engineering of new architectures [21–24], modification of thin film morphology [25–27], and interfacial engineering [28] to boost the PCEs of OPVs. Over 10% PCE has been realized from single junction bulk heterojunction (BHJ) OPVs [10,11] and over 12% PCE has been observed from triple junction BHJ OPVs (three single OPVs stacked together) [12]. In particular, interfacial engineering plays an important role in achieving such high PCEs [28].

In this short review, we will briefly introduce the role and significance of interfacial engineering in improving PCEs of BHJ OPVs. In particular, we will summarize the functions of the interfacial layers (IFLs) and the materials used as the IFLs. The operation mechanisms and the underlying physics of the IFLs in OPVs will be discussed.

Device structures and operation principles of OPVs

Figure 1 displays device structures of BHJ OPVs. In both conventional and inverted device structures, BHJ composite [23] is sandwiched between the indium tin oxide (ITO) electrode and the metal electrode to form an ITO/BHJ composite/metal sandwiched structure. The randomly distributed electron donor (D) and electron acceptor (A) have intimate contacts with the electrodes. Thus, the separated electrons and holes intend to recombine at the BHJ composite/electrode interfaces [29]. Moreover, the mismatch of the work functions of the electrodes with the energy levels of either D or A in BHJ composite would result in energy barriers for charge carrier transport, which restricts the charge carrier collection efficiency [30,31]. To circumvent these problems, the IFLs termed as either the electron extraction layer (EEL) or the hole extraction layers (HEL), according to their functionalities, are utilized to modify the BHJ composite/electrode interfaces. With the EEL and the HEL, ohmic contact is formed at the BHJ

*Corresponding author:. Gong, X. (xgong@uakron.edu)

 http://dx.doi.org/10.1016/j.mattod.2015.10.003

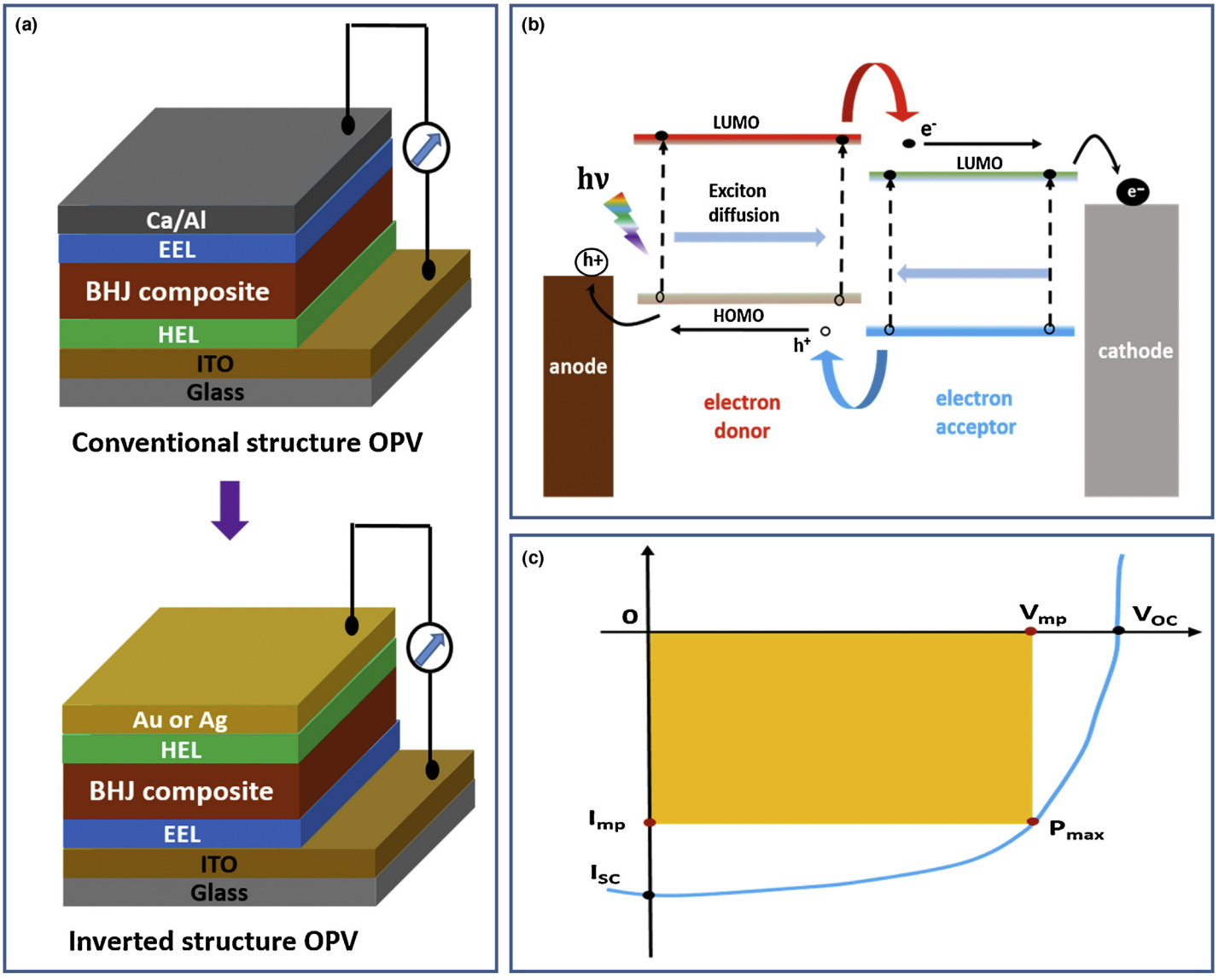

FIGURE 1

(a) Device structures of OPVs, where Ca is calcium, Al is aluminum, EEL is the electron extraction layer, BHJ is bulk heterojunction, HEL is the hole extraction layer, ITO is indium tin oxide; **(b)** Working principles of OPVs, where LUMO is the lowest unoccupied molecular orbital, HOMO is the highest occupied molecular orbital; **(c)** *I–V* characteristics of OPVs, where V_{OC} is the open-circuit voltage, I_{SC} is the short-circuit current, V_{mp} and I_{mp} is the voltage and current at maximum power, respectively, P_{max} is the maximum power of OPVs.

composite/electrode interfaces, which would reduce the energy barriers for charge transport from the BHJ composite to the corresponding electrodes. The IFLs offer charge carrier selectivity at the BHJ composite/electrode interfaces, which suppress the charge recombination at the BHJ composite/electrode interfaces [32–34]. Substantially, PCEs of OPVs with the IFLs are significantly enhanced [29]. Moreover, insertion of the IFLs in between the BHJ composite and the electrode also could tune the polarity of OPVs, allowing air stable high work function metals such as silver (Ag) or gold (Au) [35,36] to be used as the anode. Contrary to the conventional OPVs with a device structure of ITO/HEL/BHJ composite/EEL/Al, where ITO works as the anode and aluminum (Al) works as the cathode, in the inverted OPVs with a device structure of ITO/EEL/BHJ composite/HEL/Ag (or Au), ITO works as the cathode and Ag or Au works as the anode.

The basic operational principles of BHJ OPVs are shown in Fig. 1b. When the BHJ active layer is under illumination, the photonic energy is absorbed by D and/or A. The electrons are excited from the highest occupied molecular orbital (HOMO) energy levels to the lowest unoccupied molecular orbital (LUMO) energy levels of both D and/or A and the holes are left in the HOMO energy levels of D and/or A. Due to strong Columbic interactions, the electrons and the holes are bonded in pairs to form the excitons. The excitons are diffused to the D/A interface. After that, the excitons are dissociated into free electrons and holes at the D/A interface [37]. These free electrons and holes are extracted and collected by the cathode and the anode, respectively [37]. So the interface between the BHJ composite and the electrodes will determine the charge collections, which have great influences on the performance of OPVs [29,30,37].

The performance of BHJ OPVs is evaluated by the power conversion efficiency (PCE). PCE is described by PCE = $V_{OC} \times J_{SC} \times FF/P_{in}$, where V_{OC} is the open-circuit voltage, J_{SC} is the short-circuit current density, FF is the fill factor and P_{in} is the input light intensity. The FF is determined by the ratio of the maximum power from OPV to the product of V_{OC} and J_{SC}, FF = $I_{mp} \times V_{mp}/V_{OC} \times I_{SC}$, as shown in Fig. 1c, where I_{mp} and V_{mp} are the voltage and current at maximum power, respectively.

Materials for interfacial engineering

The main functions of the IFLs are highlighted as: to adjust the energy barriers between the BHJ composite and the electrodes, to select one sort of charge carriers and to reduce the interface charge carrier recombination, to tune the polarity of the electrodes and to prevent oxygen or moisture penetration into the BHJ composite/electrode interface. Currently, five types of materials have been used as the IFLs. These materials are poly(3,4-ethylenedioxythiophene):polystyrene sulfonate (PEDOT:PSS), metals, salts, metal oxides and water/alcohol soluble organic materials.

PEDOT:PSS

PEDOT:PSS is one of doped polymers. It was the first IFLs used in the development of OPVs [38], PEDOT:PSS provides an ohmic contact between the BHJ composite and the ITO electrode. PEDOT:PSS transports the holes rather than the electrons. The PEDOT:PSS thin film can smooth the surface of the ITO electrode, which reduces the linkage current, benefiting the holes being transported from the BHJ composite to the ITO anode. The features of solution processability, transparency in visible region and high electrical conductivity allow PEDOT:PSS thin layer to be widely used in OPVs [39,40]. However, it was found that the acidic PEDOT:PSS etched the ITO surface, which shortens the lifetime of OPVs [41,42]. In order to circumvent these problems, many new substitutions have been developed [30,39–42].

Metals

Thermally evaporated low work function metals including magnesium (Mg, −3.7 eV), barium (Ba, −2.7 eV) and calcium (Ca, −2.9 eV) [43,44] are also used as the IFLs in OPVs [30,43,44]. These low work function metals as the IFLs in OPVs can significantly boost PCEs of OPVs [43,44]. However, these metals are air and moisture sensitive and easy to be oxidized, which would significantly degrade the stability of OPVs. On the other hand, the thermal deposition method would enhance the costs of device fabrication, which is not suitable for large-area manufacturing. Owing to these drawbacks, the low work function metals are not widely used as the IFLs, but the studies on these IFLs provide a fundamental physics at the BHJ composite/electrode interface in OPVs.

Salts

Lithium fluoride (LiF) and cesium carbonate (Cs_2CO_3) as the IFLs are widely used in OPVs [30,45,46]. Thermally deposited LiF was firstly used to modify the interface between poly[2-methoxy-5-(3,7-dimethyloctyloxy)]-1,4-phenylenevinylene (MDMO-PPV):$PC_{61}BM$ BHJ composite and the Al cathode in the conventional OPVs. The FF was improved from 53% to 63% and the V_{OC} enlarged from 0.76 V to 0.83 V was observed from OPVs with the LiF IFL [45]. The polarity of OPVs was reversed when the Cs_2CO_3 IFL was used on the top of the ITO electrode [47]. The V_{OC} increased from 0.20 V to 0.56 V and J_{SC} increased from 7.01 mA/cm^2 to 9.70 mA/cm^2 were observed from the OPV incorporated with the Cs_2CO_3 IFL [47]. The enhanced device performance was attributed to the modified BHJ composite/electrode interface [30,48–50]. The underlying device physics of the BHJ composite/electrode interface modified by IFLs will be discussed in section 'Underlying physics of interfacial engineering'.

Metal oxides

The p-type transition metal oxides to substitute PEDOT:PSS as the HEL have been successfully introduced in OPVs to enhance its stability [33,51,52]. Thermally deposited molybdenum oxide (MoO_3) [53], nickel oxide (NiO) [54], vanadium oxide (V_2O_5) [55] and tungsten oxide (WO_3) [56] as the HELs were also reported. Comprehensive studies on these transition metal oxides as the IFLs in OPVs were reported elsewhere [57]. Nevertheless, thermal deposition process of these metal oxides is not suitable for large scale fabrication of OPVs. To overcome this obstacle, our group

TABLE 1

IFL materials, device structures and device performance parameters of conventional OPVs with IFLs.

IFLs		Device structures	Device performance				Ref.
Type of materials	Materials		V_{OC} (V)	J_{SC} (mA/cm^2)	FF (%)	PCE (%)	
Conjugated polymers	WPF-6-oxy-F	ITO/PEDOT:PSS/P3HT:$PC_{61}BM$/IFL/Al	0.62	9.89	59.0	3.67	66
	PF6NO25-py	ITO/PEDOT:PSS/PCDTBT:$PC_{71}BM$/IFL/Al	0.91	11.60	66.2	6.90	68
	PF6NO	ITO/PEDOT:PSS/PCDTBT:$PC_{71}BM$/IFL/Al	0.93	7.27	62.8	6.07	69
	PFNSO-BT	ITO/PEDOT:PSS/PTB7:$PC_{71}BM$/IFL/Al	0.65	16.76	61.1	6.61	70
	P3TMAHT	ITO/PEDOT:PSS/PCDTBT:$PC_{71}BM$/IL/Al	0.86	10.80	66.0	6.10	77
	PF2/6-b-P3TMAHT	ITO/PEDOT:PSS/PCDTBT:$PC_{71}BM$/IL/Al	0.89	10.60	67.0	6.20	77
Fullerene derivatives	bis-$PC_{61}BM$	ITO/PEDOT:PSS/PIDT-PhanQ:$PC_{71}BM$/IFL/Al	0.88	11.19	60.0	5.87	81
	bis-$PC_{61}BM$	ITO/PEDOT:PSS/PIDT-PhanQ:$PC_{71}BM$/IFL/Ag	0.88	11.50	61.0	6.22	81
	ETL-1	ITO/PEDOT:PSS/PIDT-PhanQ:$PC_{71}BM$/IFL/Ag	0.87	11.28	64.0	6.28	82
	ETL-1	ITO/PEDOT:PSS/PIDT-PhanQ:$PC_{71}BM$/IFL/Al	0.86	11.17	62.0	5.96	82
Graphene oxide and small molecule	Graphene oxide	ITO/PEDOT:PSS/P3HT:$PC_{61}BM$/IFL/Ag	0.62	10.28	62.2	3.94	87
	BA-OCH_3	ITO/PEDOT:PSS/P3HT:$PC_{61}BM$/ZnO/IFL/Al	0.65	11.61	55.0	4.21	88
	BA-CH_3	ITO/PEDOT:PSS/P3HT:$PC_{61}BM$/ZnO/IFL/Al	0.64	11.63	49.0	3.63	88
	BA-H	ITO/PEDOT:PSS/P3HT:$PC_{61}BM$/ZnO/IFL/Al	0.64	11.46	48.0	3.48	88
	BA-SH	ITO/PEDOT:PSS/P3HT:$PC_{61}BM$/ZnO/IFL/Al	0.45	10.44	42.0	1.95	88
	BA-CF_3	ITO/PEDOT:PSS/P3HT:$PC_{61}BM$/ZnO/IFL/Al	0.30	8.97	31.0	0.84	88
	BA-CN	ITO/PEDOT:PSS/P3HT:$PC_{61}BM$/ZnO/IFL/Al	0.27	8.15	28.0	0.62	88

demonstrated a facile route to solution-processed MoO_x HEL at room temperature in OPVs [58]. The OPVs with the MoO_x HEL possessed even higher PCEs compared to that with PEDOT:PSS HEL. We also observed comparable device performance from the OPVs incorporated with magnetic iron oxide (Fe_3O_4) nano-particles as an efficient HEL [59].

The n-type solution-processed zinc oxide (ZnO_x) [60,61] and titanium oxide (TiO_x) [62] were also used as the efficient EELs in the inverted OPVs due to their good transparency and electron selectivity [60–63]. The low energy offset between the LUMO energy level of the ZnO_x EEL and the LUMO energy level of the electron donors would reduce the energy barrier for the electrons being transported from the BHJ composite to the corresponding cathode, resulting in enhanced PCEs [60–63].

Water/alcohol soluble organic materials

The organic materials with side chains, such as amino, phosphate, carboxyl, quaternary ammonium, sulfonic and zwitterionic groups, would possess good solubility either in water or alcohol solvents [64,65]. These water/alcohol soluble organic materials possess the advanced features that their electrical properties are tunable through structural modification. Moreover, as the IFLs, its can be deposited on the top of or underneath of BHJ composite without damage either BHJ composite or itself due to its water/alcohol solubility.

TABLE 2

IFL materials, device structures and device performance parameters of inverted OPVs with IFLs.

IFLs		Device structures	Device performance				Ref.
Type of materials	**Materials**		**V_{OC} (V)**	**J_{SC} (mA/cm^2)**	**FF (%)**	**PCE (%)**	
Conjugated polymers	WPF-6-oxy-F	ITO/IFL/P3HT:PC_{61}BM/PEDOT:PSS/Ag	0.65	8.83	59.0	3.38	67
	PFN-Br	ITO/ZnO/IFL/PBDT-DTNT:PC_{71}BM/MoO_3/Al	0.75	17.40	61.0	8.40	72
	PFN	ITO/IFL/PTB7:PC_{71}BM/MoO_3/Ag	0.75	17.46	69.9	9.21	73
	PFN-OX	ITO/IFL/PBDT-DTNT:PC_{71}BM/MoO_3/Al	0.74	17.62	66.1	8.62	76
Non-conjugated polyelectrolytes	PEIE	ITO/IFL/P3HT:ICBA/MoO_3/Al	0.81	11.00	66.0	5.90	78
	Polyethlyeneimine	ITO/IFL/PTB7:PC_{71}BM/PEDOT:PSS/Ag	–	–	–	~6.00	79
	Polyallyamine	ITO/IFL/PTB7:PC_{71}BM/PEDOT:PSS/Ag	–	–	–	~6.00	79
Fullerene derivatives	C-PCBSD	ITO/ZnO/IFL/P3HT:PC_{61}BM/PEDOT:PSS/Ag	0.60	12.80	58.0	4.40	83
	C-PCBSD	ITO/ZnO/IFL/P3HT:ICBA/PEDOT:PSS/Ag	0.84	12.40	60.0	6.22	84
	PC_{60}BM-G2	ITO/ZnO/IFL/PBDT-DTBT:PC_{71}BM/MoO_3/Al	0.73	14.00	62.8	6.42	96

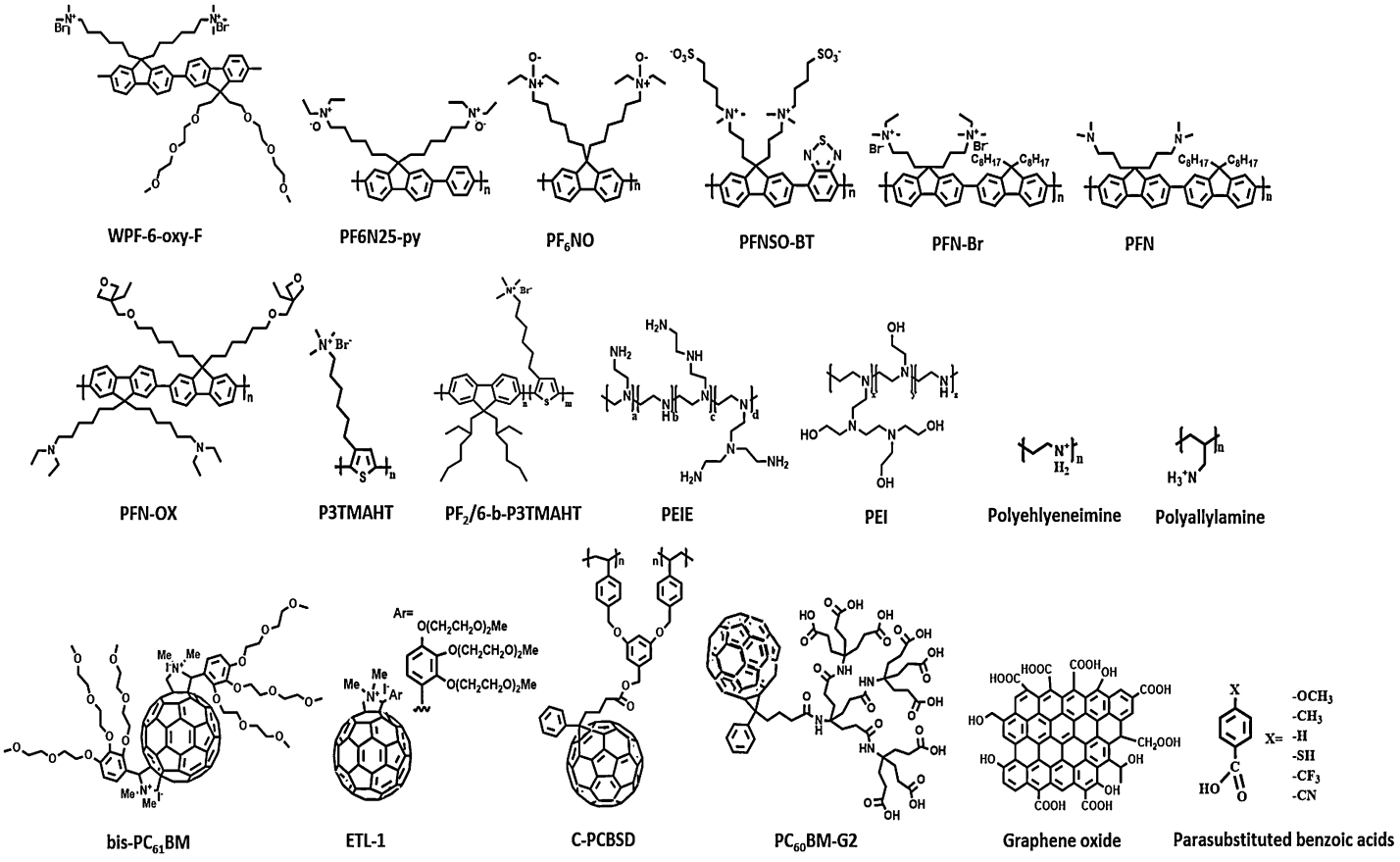

SCHEME 1

Molecular structures of organic materials used as the interfacial layers in OPVs.

Tables 1 and 2 summarize four types of water/alcohol soluble organic materials used as the IFLs in both conventional and inverted OPVs. Their molecular structures are presented in Scheme 1.

The first one is conjugated polymers. Oh et al. observed nearly 60% enhanced PCEs from P3HT:$PC_{61}BM$ based OPVs incorporated with poly[(9,9-bis((6′-(N,N,N-trimethylammonium)hexyl)-2,7-fluorene)-alt-(9,9-bis(2-(2-(2-methoxyethoxy)ethoxy)ethyl)-9-fluorene))] dibromide (WPF-6-oxy-F) as the cathode IFL [66]. They further found out that enhanced PCEs was solely resulted from the increased V_{OC} [66,67]. Later on, novel polyfluorene derivatives, such as PF6NO25-py [68], PF_6NO [69], PFNSO-BT [70], PFN-Br [71,72], PFN [73], were also applied as the IFLs to enhance PCEs of OPVs [74,75]. Among these polyfluorene derivatives, poly[(9,9-bis(3′-((N,N-dimethyl)-N-ethylammonium)-propyl)-2,7-fluorene)-alt-2,7-(9,9-dioctylfluorene)] dibromide (PFN-Br) was the most widely used IFL in OPVs. In 2012, our group applied PFN-Br to reengineer the ZnO_x EEL in the inverted OPVs and observed increased V_{OC}, J_{SC} and FF, consequently, enhanced PCE [72]. Late one, Cao et al. reported a PCE of 9.2% from the inverted OPV incorporated with poly[(9,9-bis(3′-(N,N-dimethylamino)propyl)-2,7-fluorene)-alt-2,7-(9,9-dioctylfluorene)] (PFN) as the EEL [73]. We further reported efficient inverted OPVs with over 1 μm thickness of BHJ composite by using poly[(9,9-bis(6′-(N,N-dimethylamino)propyl)-2,7-fluorene)-alt-2,7-(9,9-bis(3-ethyl(oxetane-3-ethyloxy)-hexyl)-fluorene)] (PFN-OX) as the EEL [76]. Our finding resolved one of bottleneck problems for large-scale fabrication of OPVs by roll-to-roll technique [76].

It was also demonstrated that polythiophene derivatives could be used as the effective EELs to enhance PCEs (V_{OC} and J_{SC}) in the conventional OPVs. For example, improved PCEs of 6.1% and 6.2% were observed from the OPVs with P3TMAHT and PF2/6-b-P3TMAHT as the EELs, respectively [77].

The second one is non-conjugated polyelectrolytes. Kippelen et al. demonstrated that polyethylenimineethoxylated (PEIE) or branched polyethylenimine (PEI) as the IFLs to tune the energy alignment at the BHJ composite/electrode interface effectively,

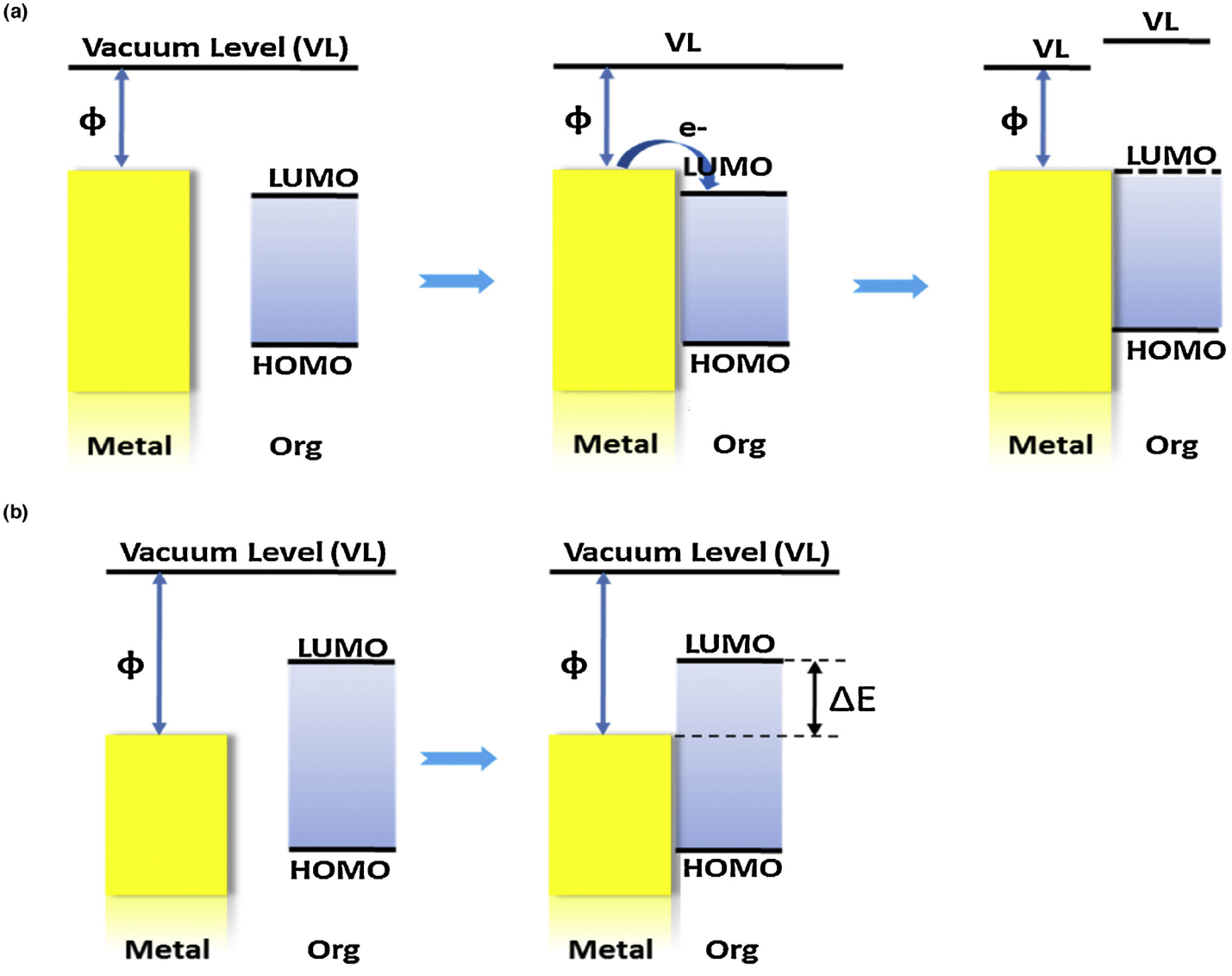

FIGURE 2

(a) Metal/organic materials (Org) with Fermi contact; **(b)** Metal/organic materials with energy barriers. Φ represents the work function of the electrode. Δ*E* represents the height of the energy barrier.

resulting in enhanced PCEs in the inverted OPVs [78]. Polyethyleneimine and polyallyamine [79] were also reported as the IFLs in enhancing PCEs of OPVs.

The third one is fullerene derivatives [80]. Jen et al. found that OPVs with bis-$PC_{61}BM$ EELs exhibited greatly enhanced V_{OC} and J_{SC} [81,82]. Hsu et al. also found that a cross-linkable fullerene material, [6,6]-phenyl-C_{61}-butyric styryldendron ester (C-PCBSD) with ZnO_x as the EELs could reduce the contact resistance at the BHJ composite/electrode interface, thereby suppress the leakage pathways of the ZnO_x EEL [83], resulting in over 6.2% enhanced PCEs from ICBA:P3HT based OPVs [84].

Last but not the least is graphene oxide and other small molecular materials. Li et al. found that graphene oxide as the HEL could significantly enhance PCEs of OPVs [85–87]. The enhanced PCEs were attributed to ohmic contact between the BHJ composite and the anode [87]. Jen et al. also demonstrated parasubstituted benzoic acids with various substitute groups as the IFLs in OPVs [88]. By tuning the substitute group, the dipole moments with different strengths could be formed at the BHJ composite/electrode interface [88].

Underlying physics of interfacial engineering

The BHJ composite/electrode interface

Figure 2 proposes the operational principles at the BHJ composite/electrode interface. Before the metal electrode and organic materials get intimate contact, the LUMO and HOMO energy levels of organic materials and the work function of the metal electrode remain at their original values. After contacting, the energy levels alignment at the metal/organic materials interface would take place. If the work function of the metal electrode is higher than the LUMO energy level of organic materials, the electrons will be transported from the metal electrode to organic materials due to the electro-potential [89]. The energy level at metal electrode surface will pin to the LUMO energy level of organic materials, which is termed as ohmic contact or Fermi level pining. Such ohmic contact will minimize the energy barriers for charge carrier transport at the BHJ composite/electrode interface. So, enhanced PCEs from OPVs are expected. On the other hand, if the work function of the metal electrode is lower than the LUMO energy level of organic materials, the electron will be transported from organic materials to the metal electrode due to different electro-potentials [89]. An electric field with the direction pointing from organic materials to the metal electrode will be formed. Such electric field would create an energy barrier for the electrons being transported from organic materials to the metal electrode, which is deteriorating charge collection efficiency in OPVs [89,90].

The BHJ composite/electrode interface modified by IFLs

In general, PEDOT:PSS, metals, salts, and metal oxides as the IFLs can improve charge transport properties at the BHJ composite/electrode interface. The ITO electrode has a work function of −4.7 eV [6], which is higher than the HOMO energy levels of most organic materials. The work function of PEDOT:PSS is −5.0 eV [38]. With PEDOT:PSS on the surface of the ITO electrode, the energy barriers between the ITO electrode and organic materials would be suppressed and Fermi contact would be formed. Consequently, OPVs with improved PCEs are expected [38].

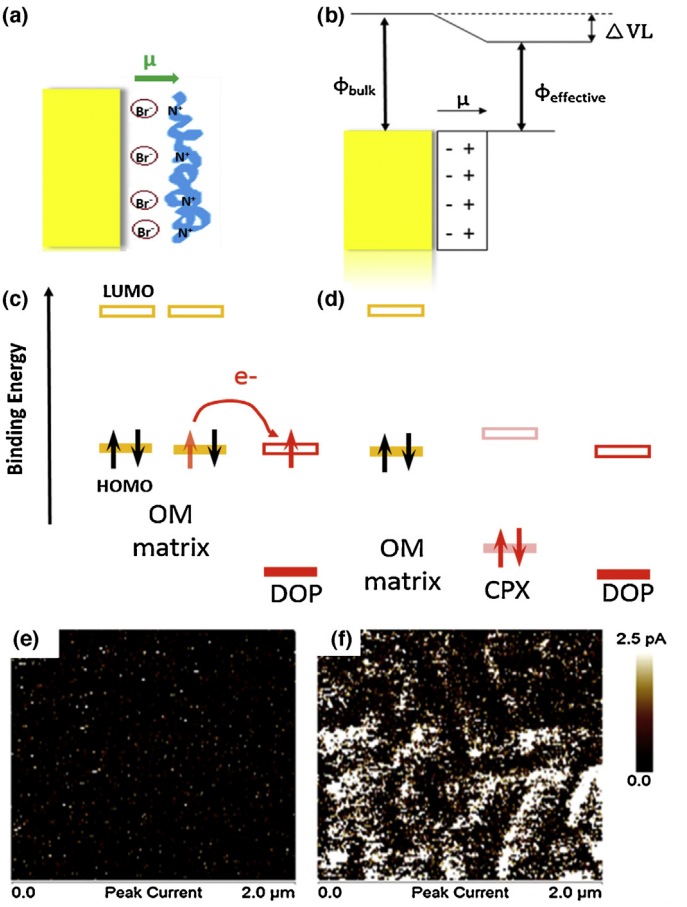

FIGURE 3

(a) Dipole moment formation on the surface of the electrode by PFN-Br; **(b)** Reduced surface work function of the electrode by the dipole moment; **(c)** Standard model for molecular electrical doping assuming integer charge transfer from the HOMO energy level of organic molecule (OM) to the LUMO energy level of the p-dopant (DOP) leading to ionized molecules; **(d)** Alternative model assuming the hybridization of the frontier molecular orbitals of the OM and the p-dopant in a supramolecular complex; surface current densities of **(e)** ZnO; and **(f)** $PC_{60}BM$-G2/ZnO measured by the conductive peak force tapping tunneling AFM.

The aluminum (Al) electrode has a work function of −4.4 eV, which is lower than the LUMO energy level (−4.0 eV) of fullerenes derivatives [13]. Insertion of a low work function metal, such as Ba (−2.7 eV) [43], Ca (−2.9 eV) [44], Mg (−3.7 eV) [44], between the BHJ composite and Al electrode, the energy barriers for electron extraction from the BHJ composite to Al electrode can be reduced. Therefore, significantly increased V_{OC}, FF and J_{SC} are expected.

Salts based IFLs were reported to have three effects in improving the BHJ composite/electrode interface in OPVs. The salts, e.g. LiF, could work as a buffer layer to prevent the BHJ composite from damage during the thermal deposition process of the top electrode [32]. The permeant dipole moment in salts would contribute to the improved PCEs in OPVs. The formation of Li–F or Cs–O dipole moment at the BHJ composite/electrode interface significantly reduced surface work functions of the electrode [46,47], therefore, the energy barriers for electron extraction by the electrode were suppressed. The salts were also reported as the dopants when used as the IFLs in OPVs. The doped BHJ composite by Li^+ or Cs^{2+} ions

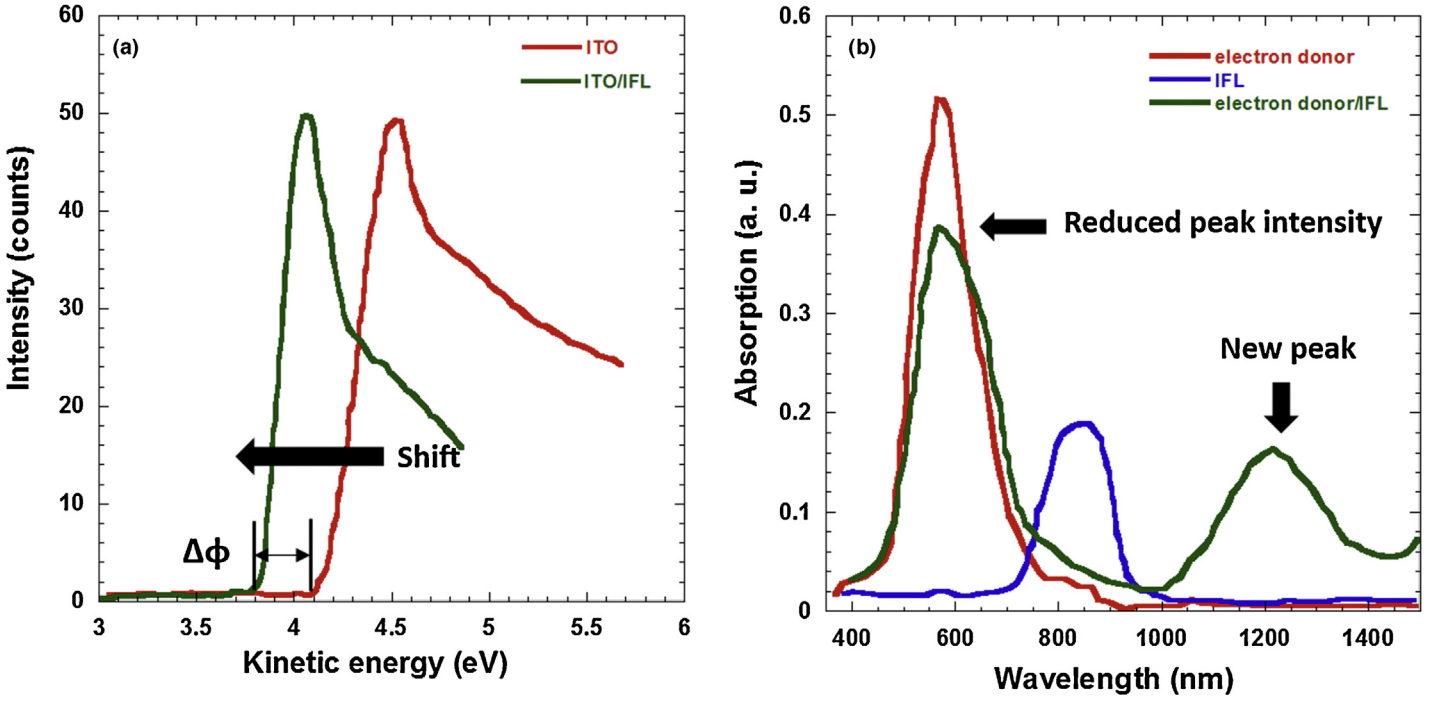

FIGURE 4

(a) Shift of work function of ITO due to the IFL, characterized by UPS. ΔΦ is the shift of work function; **(b)** Doping of the electron donor in the BHJ composite by the IFL characterized by absorption spectroscopy.

from the salts will form Fermi contact with the electrode to reduce the energy barriers [48–50], resulting in increased V_{OC} and FF.

Metal oxides, MoO_3 [53], NiO [54], V_2O_5 [55] and WO_3 [56] with low HOMO energy levels can effectively reduce the energy barriers for charge transport at the BHJ composite/ITO electrode interface, resulting in enhanced PCEs. The n-type metal oxides, ZnO_x, TiO_x, with higher LUMO energy levels than those of the electron acceptor in the BHJ composite, can minimize the energy barriers for the electrons being extracted from BHJ composite to the corresponding cathode, resulting in enhanced PCEs [60–62]. Moreover, the charge separation at the interface between these n-type metal oxides and the BHJ composite also has great contributions to increased J_{SC} [83,84]. Comprehensive reviews on the contacts between metal oxides and organic materials were reported elsewhere [91,92].

However, due to the low electrical conductivity and the light absorption in the visible region, solution-processed metal oxides as the HELs have to be ultrathin, which results in a great challenge on the understanding of underlying physics of enhanced PCEs. Based on our studies of the origins of enhanced PCEs of OPVs with MoO_x, ZnO and Fe_3O_4, we found that the enhanced surface electrical conductivities of metal oxides play an important role in enhanced PCEs of OPVs [58,59].

Enhanced PCEs by water/alcohol soluble organic materials as the IFLs

Figure 3a,b illustrate the shift of the vacuum energy level at the metal surface due to the dipole moment. With the dipole moment (μ) pointing outwards the electrode surface, the effective vacuum level at the electrode surface could be reduced. Then, the effective work function at the surface of the metal electrode could be sufficiently reduced, which is favorable for the formation of ohmic contact at the BHJ composite/electrode interface. It was proposed that enhanced PCEs of OPVs, especially the increased V_{OC}, was resulted from the dipole moment formed at the BHJ composite/electrode interface [64–67,79–81], for example, polyfluorene derivatives, PEIE, PEI, Bis-$PC_{61}BM$, or the IFLs possess strong internal dipole moment [30,45,46,64–67,72,79–81].

Another explanation for enhanced PCEs was that the BHJ composite was doped by the IFLs [30,85–87]. As a result, ohmic contact between the BHJ composite and the electrode was generated, resulting in both increased V_{OC} and J_{SC} in OPVs [86,87]. Figure 3c,d display two proposed doping mechanism of IFL as chemical dopants. The IFL dopant has a low lying LUMO energy level which is comparable to the HOMO energy level of organic materials, thus, the electrons in the HOMO energy level of organic materials are transferred to the LUMO energy level of the IFL dopant, resulting in a complex with lower Fermi level [93]. Owing to the low-lying Fermi level of the complex, ohmic contact between the BHJ composite and anode interface was formed [93,94].

Due to the effects of the dipole moment, the binding energies between the electrons at the surface of the electrode and those in the bulk electrode are changed. Therefore, the modified surface work function of the electrode via the dipole moment and/or the changed energy levels of organic materials by the IFL dopant were characterized by ultraviolet photoemission spectroscopy (UPS), as shown in Fig. 4a [72,80,95]. The doping of organic materials in the BHJ composite by the IFL dopant was measured by the light absorption spectroscopy [87,93,94]. Due to the doping process, the bandgap of the electron donors could be reduced and the

polarons could be generated [94]. The polarons generally have different light absorptions compared to that of the conjugated backbone of the electron donors, which is in the range from 700 nm to 1000 nm, thus, new peak will appear in the absorption spectra, as shown in Fig. 4b. However, due to the ultrathin IFLs, the exact origins of enhanced PCEs are hard to be distinguished from the dipole moment, doping process or even both of these two mechanisms.

In addition to the mechanisms discussed above, our group found that surface electrical conductivity of the IFLs plays an important role in enhanced PCEs [72,96]. In order to further verify it and avoid the influences from doping and the dipole moment, we designed a novel neutral fullerene derivative ($PC_{60}BM$-G2) as the IFL [96], which possesses almost the same LUMO energy level to that of $PC_{71}BM$. The domain of peak of TUNA currents flowing on the ZnO EEL was increased after modified by $PC_{60}BM$-G2 EEL, which indicated that surface electrical conductivity at the ZnO EEL was greatly increased, as shown in Fig. 3e,f. Contributed by enhanced surface electrical conductivities, without changing the V_{OC}, the overall PCEs was increased from 4.77% to 6.42% [96]. Moreover, our studies on enhanced PCEs of OPVs with room-temperature solution-processed MoO_x and magnetic Fe_3O_4 IFLs also indicated that the increased PCEs were originated from the enhanced surface electrical conductivities of the IFLs [58,59].

Prospects and outlook

The state-of-art PCEs of OPVs have overcome the commercialization criteria-10%. Novel materials development, thin film morphology optimization, and interfacial engineering are still ongoing directions to further boost PCEs of OPVs. Among them, interfacial engineering by the IFLs is still a simple and practical route to approach high PCEs. The materials used as the IFLs should possess effective charge carrier transport properties, fine-tuning the energy level alignments at the BHJ composite/electrode interface and high electrical conductivity. Moreover, the materials as the IFLs are expected to have a good solubility in water/alcohol or non-halogen solvents, which allow them to be solution-processed either on the top of and underneath of BHJ composite, and to possess high air and moisture stability, for example, cross-linkable IFLs to enhance the stability of OPVs.

Acknowledgement

The authors would like to thank NSF and Air Force Research for financial support.

References

[1] D.M. Chapin, et al. J. Appl. Phys. 25 (1954) 676.
[2] T. Saga, NPG Asia Mater. 2 (2010) 96.
[3] E.D. Coyle, et al., Understanding the Global Energy Crisis, Purdue University Press, 2014.
[4] Y.-W. Su, et al. Mater. Today 15 (2012) 554.
[5] S. Gunes, et al. Chem. Rev. 107 (2007) 1324.
[6] G. Li, et al. Nat. Mater. 4 (2005) 864.
[7] A.C. Mayer, et al. Mater. Today 10 (2007) 28.
[8] Y. Sun, et al. Nat. Mater. 11 (2012) 44.
[9] G. Li, et al. Nat. Photonics 6 (2012) 153.
[10] Y. Liu, et al. Nat. Commun. 5 (2014) 5293.
[11] C. Liu, et al. ACS Appl. Mater. Interfaces 7 (2015) 4928.
[12] C.C. Chen, et al. Adv. Mater. 26 (2014) 5670.
[13] Y. Liang, et al. Adv. Mater. 22 (2010) E135.
[14] X. Guo, et al. Nat. Photonics 7 (2013) 825.
[15] Y. Li, Acc. Chem. Res. 45 (2012) 723.
[16] Z.B. Henson, et al. Nat. Chem. 4 (2012) 699.
[17] A. Mishra, et al. Angew. Chem. Int. Ed. 51 (2012) 2020.
[18] T. Xu, et al. Mater. Today 17 (2014) 11.
[19] M.C. Scharber, et al. Prog. Polym. Sci. 38 (2013) 1929.
[20] J. Roncali, et al. Adv. Mater. 26 (2014) 3821.
[21] K.-S. Liao, et al. Energies 3 (2010) 1212.
[22] C.W. Tang, Appl. Phys. Lett. 48 (1986) 183.
[23] H.-Y. Chen, et al. Nat. Photonics 3 (2009) 649–653.
[24] G. Yu, et al. Science 270 (1995) 1789.
[25] W. Ma, et al. Adv. Funct. Mater. 15 (2005) 1617.
[26] J. Peet, et al. Nat. Mater. 6 (2007) 497.
[27] C. Yi, et al. J. Mater. Chem. C 3 (2015) 26.
[28] L. Chen, et al. Adv. Mater. 21 (2009) 1434.
[29] N.S. Sariciftci, et al. Science 258 (1992) 1474.
[30] R. Steim, et al. J. Mater. Chem. 20 (2010) 2499.
[31] S.K. Hau, et al. Appl. Phys. Lett. 92 (2008) 253301.
[32] L.M. Chen, et al. J. Mater. Chem. 20 (2010) 2575.
[33] S. Chen, et al. J. Mater. Chem. 22 (2012) 24202.
[34] H. Zhou, et al. Adv. Mater. 25 (2013) 1646.
[35] C. Yi, et al. Curr. Opin. Chem. Eng. 2 (2013) 125.
[36] J.H. Seo, et al. J. Am. Chem. Soc. 130 (2008) 10042.
[37] C. Waldauf, et al. Appl. Phys. Lett. 89 (2006) 233517.
[38] L.S. Roman, et al. Adv. Mater. 10 (1998) 774.
[39] Z. Hu, et al. Solar Energy Mater.: Solar Cells 95 (2011) 2763.
[40] D. Gupta, et al. Adv. Mater. 3 (2013) 782.
[41] M. Jorgensen, et al. Sol. Energy Mater. Sol. Cells 92 (2008) 682.
[42] M. Jorgensen, et al. Adv. Mater. 24 (2012) 580.
[43] M.O. Reese, et al. Appl. Phys. Lett. 92 (2008) 053307.
[44] H.B. Michaelson, J. Appl. Phys. 48 (1977) 4729.
[45] C.J. Brabec, et al. Appl. Phys. Lett. 80 (2002) 1288.
[46] G. Li, et al. Appl. Phys. Lett. 88 (2006) 253503.
[47] J. Huang, et al. Adv. Mater. 20 (2008) 415.
[48] T.M. Brown, et al. Appl. Phys. Lett. 77 (2000) 3096.
[49] L.S. Hung, et al. Appl. Phys. Lett. 70 (1997) 152.
[50] S.E. Shaheen, et al. J. Appl. Phys. 84 (1998) 2324.
[51] T. Yang, et al. Adv. Energy Mater. 2 (2012) 523.
[52] F. Wang, et al. Energy Environ. Sci. 8 (2015) 1059.
[53] V. Shrotriya, et al. Appl. Phys. Lett. 88 (2006) 073508.
[54] M.D. Irwin, et al. Proc. Natl. Acad. Sci. U. S. A. 105 (2008) 2783.
[55] J. Huang, et al. Org. Electron. 10 (2009) 1060.
[56] C. Tao, et al. Appl. Phys. Lett. 94 (2009) 043311.
[57] J. Meyer, et al. Adv. Mater. 24 (2012) 5408.
[58] B. Li, et al. ACS Photonics 1 (2014) 87.
[59] K. Wang, et al. ACS Appl. Mater. Interfaces 5 (2013) 10325.
[60] T. Yang, et al. J. Phys. Chem. C 114 (2010) 6849.
[61] M.S. White, et al. Appl. Phys. Lett. 89 (2006) 143517.
[62] A. Hayakawa, et al. Appl. Phys. Lett. 90 (2007) 163517.
[63] S. Lattante, Electronics 3 (2014) 132.
[64] F. Huang, et al. Chem. Soc. Rev. 39 (2010) 2500.
[65] C. Duan, et al. Chem. Soc. Rev. 42 (2013) 9071.
[66] S.-H. Oh, et al. Adv. Funct. Mater. 20 (2010) 1977.
[67] S.-I. Na, et al. Appl. Phys. Lett. 97 (2010) 223305.
[68] X. Guan, et al. Adv. Funct. Mater. 22 (2012) 2846.
[69] Z. Hu, et al. Chem. Commun. (2015).
[70] C. Duan, et al. Chem. Sci. 4 (2013) 1298.
[71] J.H. Seo, et al. Adv. Mater. 21 (2009) 1006.
[72] T.B. Yang, et al. Energy Environ. Sci. 5 (2012) 8208.
[73] Z. He, et al. Nat. Photonics 6 (2012) 593.
[74] C.M. Zhong, et al. Chem. Mater. 23 (2011) 4870.
[75] Y. Dong, et al. Adv. Mater. 25 (2013) 3683.
[76] X.W. Hu, et al. Adv. Energy Mater. 4 (2014) 1400378.
[77] J.H. Seo, et al. J. Am. Chem. Soc. 133 (2011) 8416.
[78] Y. Zhou, et al. Science 336 (2012) 327.
[79] H. Kang, et al. Adv. Mater. 24 (2012) 3005.
[80] J. Zhou, et al. J. Am. Chem. Soc. 135 (2013) 8484.
[81] K.M. O'Malley, et al. Adv. Energy Mater. 2 (2012) 82.
[82] C.-Z. Li, et al. J. Mater. Chem. 22 (2012) 8574.
[83] C.H. Hsieh, et al. J. Am. Chem. Soc. 132 (2010) 4887.
[84] Y.-J. Cheng, et al. J. Am. Chem. Soc. 132 (2010) 17381.
[85] S.S. Li, et al. ACS Nano 4 (2010) 3169.
[86] Y. Gao, et al. Appl. Phys. Lett. 97 (2010) 203306.

[87] Y. Gao, et al. Adv. Mater. 23 (2011) 1903.
[88] H.-L. Yip, et al. Adv. Mater. 20 (2008) 2376.
[89] H. Ishii, et al. Adv. Mater. 11 (1999) 605.
[90] S. Braun, et al. Adv. Mater. 21 (2009) 1450.
[91] M.T. Greiner, et al. Nat. Mater. 11 (2012) 76.
[92] L. Ley, et al. Adv. Funct. Mater. 23 (2013) 794.
[93] H. Mendez, et al. Angew. Chem. Int. Ed. 52 (2013) 7751.
[94] B. Lussem, et al. Phys. Status Solidi A 210 (2013) 9.
[95] L. Gao, Mater. Sci. Eng. Rep. 68 (2010) 39.
[96] C. Yi, et al. ACS Appl. Mater. Interfaces 6 (2014) 14189.